Condensed Plasmas under Microgravity

G. E. Morfill,[1] H. M. Thomas,[1] U. Konopka,[1] H. Rothermel,[1] M. Zuzic,[1] A. Ivlev,[1] and J. Goree[2]

[1]*Max-Planck-Institut für extraterrestrische Physik, 85740 Garching, Germany*
[2]*University of Iowa, Department of Physics and Astronomy, Iowa City, Iowa 52242*

Experiments under microgravity conditions were carried out to study "condensed" (liquid and crystalline) states of a colloidal plasma (ions, electrons, and charged microspheres). Systems with $\sim 10^6$ microspheres were produced. The observed systems represent new forms of matter—quasineutral, self-organized plasmas—the properties of which are largely unexplored. In contrast to laboratory measurements, the systems under microgravity are clearly three dimensional (as expected); they exhibit stable vortex flows, sometimes adjacent to crystalline regions, and a central "void," free of microspheres.

"Colloidal plasmas" may undergo phase transitions and condense to form "liquid plasmas" and "plasma crystals" [1–9]. These plasma states are not normal condensed matter states—the individual plasma components (electrons, ions, microspheres) coexist in an ordered (or organized) structural form, which arises as a consequence of the strong Coulomb coupling between them—they therefore represent new states of matter. Research into the properties of these new plasma states, e.g., the thermodynamics, microscopic, and collective processes, benefits from the fact that one plasma component, the microspheres, may be visualized and analyzed at the kinetic level. The charged microspheres are crucial; without them the "plasma condensation" would not occur [10]. However, there exists a major constraint—gravity. The external gravitational pressure restricts laboratory investigations to a limited range of state variables. Consequently, it was recognized fairly early that microgravity measurements were needed to complement laboratory research [1,11,12]. Experiments in space have now been performed in a radio-frequency (rf) discharge colloidal plasma, and the first results are presented together with a discussion of the salient features observed.

In order to appreciate the scope of microgravity research for this fundamental physics field, we summarize some of the relevant issues: On Earth, the microspheres have to be electrostatically supported against gravity. The electric fields required are $E = 10$ V/cm for particles of mass $m \approx 10^{-10}$ g and charge $Q = 10^4 e$. Such strong fields occur in plasma boundary layers, e.g., the sheath above the electrodes, and are characterized by supersonic ion flows and nonequilibrium conditions. Over a lattice separation, Δ, the (unavoidable) electric bulk force in this sheath varies by an amount $\Delta F \approx Q \frac{dE}{dz} \Delta$, which is comparable to the interparticle forces Q^2/Δ^2. This and the ion drag have a profound influence on liquid flow properties and crystal structures. Gravity also causes "crystal crushing" as well as shear forces and therefore prevents the establishment of large 3D crystals or liquids (see [11]). The internal pressure generated by n_L lattice planes is $P_g \approx Q/\Delta \frac{dE}{dz}(n_L - 1)$. It is clear that the existence of such large body forces makes it difficult, if not impossible, to investigate experimentally whether "plasma crystals" have self-confining binding forces [13–15] and whether "plasma fluids" have properties such as surface tension. Finally, the detailed determination of system properties—in particular the thermodynamics, phase transitions, and flow dynamics—requires investigations over a large range of "parameter space" (e.g., the "coupling parameter" $\Gamma = Q^2/4\pi\varepsilon_0\Delta kT =$ Coulomb energy/thermal energy and the "structure parameter" $\kappa = \Delta/\lambda_D =$ mean particle separation/Debye length of the plasma) in order to understand the equation of state of condensed plasmas [16]. While in principle the charge, Q, and hence Γ, can be varied quite easily, gravity constrains this in practice through the levitation requirement ($mg = QE$). The same is true for κ, which is governed by the external pressure acting on the system—and which is again constrained by the action of gravity.

In the absence of gravity, microspheres can in principle be embedded in the main plasma, where the major bulk forces—electric fields, $Q\mathbf{E}$, thermophoresis, $\mathbf{F}_{th}$, density gradients $\mathbf{F}_{gr}$, ion drag, $\mathbf{F}_i$, and neutral drag, $\mathbf{F}_n$—are much smaller. $\mathbf{F}_{th}$ and $\mathbf{F}_i$ are directed outwards, $Q\mathbf{E}$ and $\mathbf{F}_{gr}$ into the main plasma, and $\mathbf{F}_n$ is a friction force slowing the particles down. In the main plasma, the ion drag force is due to subsonic drifts, $\mathbf{v}_i$, governed by collisions with neutrals at the rate $\mathbf{v}_{in}$. Throughout the subsonic ion drift regime of the main plasma we get the interesting result that the ratio of the bulk forces for a particle at rest is

$$|\mathbf{F}/Q\mathbf{E}| = 8.06 \times 10^{-12}(n_i/P_{mb}T_{300})a_\mu f_e \equiv \xi, \quad (1)$$

i.e., it depends only on neutral gas pressure (P_{mb} in millibar), ion temperature (in units of 300 K), ion density (cm^{-3}), and particle size a_μ (in microns). f_e is the cross section enhancement due to ion-microsphere Coulomb collisions [17]. Hence for particles in the micron size range, it should be possible under microgravity conditions

to adjust the system to be largely force free ($\xi = 1$) provided $\mathbf{F}_{th}$ and $\mathbf{F}_{gr}$ can be kept small. If (1) is smaller than unity, the microspheres will then aggregate in the main plasma under the external confining force $Q\mathbf{E}$, and can thus then be controlled easily. The μg environment is very different from the gravity dominated one in the laboratory, enabling research in a wide parameter range not accessible on Earth.

Our "space plasma crystal" experiment is shown schematically in Fig. 1, including the viewing geometry. So far, this plasma chamber has been flown in 51 parabolic test flights on aircraft (typically 10^{-2} g for time periods of 10 to 15 sec) and twice on a sounding rocket. It is the latter experiment which we report on here. Microspheres are injected into the plasma near apogee when the ballistic flight phase is reached and atmospheric drag is small. The residual gravitational field is then a few μg for about 6 min. Because of these flight time limitations only a few investigations could be performed. Bearing in mind the above mentioned constraints imposed by gravity, priority was given to the production and investigation of a 3D plasma condensation.

A selection of the results is summarized in Figs. 2 and 3. It is seen that under microgravity conditions three-
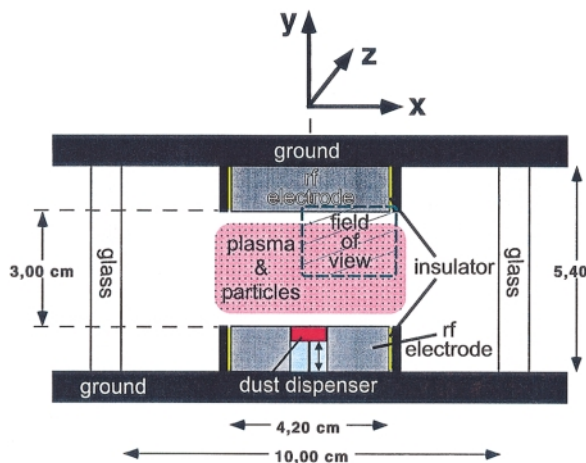

FIG. 1 (color). The space experiments were performed in a low pressure, low temperature radio-frequency (rf) discharge chamber, employing a symmetrical parallel plate reactor installed in a glass cylinder. Overall dimensions: diameter 13.6 cm, height 7 cm. The electrode dimensions are given in the figure, providing a cylindrical plasma regime of diameter $\sim$5 cm and height $\sim$3 cm. A piston operated dust dispenser, covered by a wire mesh of size 20 μm, is inserted into the center of the lower electrode. Monodisperse polymer particles of diameter 14.9 μm can be injected into the plasma by remote command. The gas in the plasma chamber is krypton, the operating pressure is 0.4 mbar. The rf power can be varied by telecommand to change the plasma environment. The particles are illuminated by a vertically arranged thin sheet of laser light (sheet thickness about 100 μm), and visualized using a CCD video camera. Both camera and laser can be moved horizontally to obtain a 3D image of the particle cloud. The field of view is indicated—it covers roughly $\frac{1}{4}$ of the system, which was assumed to be cylindrically symmetric.

dimensional plasma condensations are indeed formed. The condensations are spheroidal and contain about a million particles, arranged around a central particle "void." The existence of such a void implies that $|\mathbf{F}_i + \mathbf{F}_{th}| > |Q\mathbf{E} + \mathbf{F}_{gr}|$ in the central plasma for our experimental conditions. This finding is investigated in more detail: experimentally by using single particles as tracers of the force field, theoretically by employing the results of plasma simulations (siglo 2D, [18]). The results are the following: (i) Microspheres embedded in a pure e, i plasma move out from the center but do not follow the computed electric field. This appears to rule out $\mathbf{F}_i$ as the dominant force. Computations show that for our experimental conditions $\mathbf{F}_i/Q\mathbf{E} \approx 0.1$, which confirms this. (ii) Microspheres embedded in the void also move outwards [Fig. 4]. Integrating the equation of motion

$$m d\mathbf{v}/dt = \sum_k \mathbf{F}_k, \qquad (2)$$

and substituting appropriate experiment conditions (e.g., gas pressure, temperature) allows us to derive the net outward force, $\mathbf{F}$, from the measured particle trajectories. In the inner region of the void $\mathbf{F} = (1.0 \pm 0.1) \times 10^{-7}$ dyne and in the outer region $\mathbf{F} = (3.2 + 1.0) \times 10^{-7}$ dyne. For comparison, the computed inward directed electrostatic force is $\sim 3 \times 10^{-8}$ dyne and $\sim 10^{-7}$ dyne, respectively.

This pinpoints the thermophoretic force as the most important component. Reducing power (and hence heating) results in a decrease of the void (see Figs. 2 and 3), which may be taken to support this conclusion. If this is correct, the temperature gradient of the neutral gas in the plasma chamber is of the order 1 K/cm.

Next the dynamics of the condensed plasma is investigated by looking at the particle trajectories over a sufficiently long time of O (seconds). The measurements show that the system behaves like a convective fluid with stable "vortice flows" or "fluid cells." A horizontal scan confirms that these fluid cells have a toroidal geometry, which probably extends over 2π in azimuth. (We cannot be completely certain because we observed only one quadrant.) Azimuthal rotation, if it exists, is slow—from the time the microspheres remain in the narrow sheet of laser light we estimate a rotation period $T \geq 4000$ sec.

Vortice flows are not expected to occur, if only conservative forces exist. Hence possible driving mechanism(s) could be due to changes in the microspheres' charge, to ion drag, or thermophoretic forces. Our previous discussion suggests that the process might be associated with the spatially varying thermophoretic force, if this is indeed the dominant component for $\mathbf{F}$. Returning to Fig. 4, we see that the net force acting on the individual particles in the void is stronger (longer trajectories) in the vertical direction than along the midplane of the chamber. This net force provides a torque and could initiate a poloidal vortex flow provided the fluid is sufficiently strongly coupled
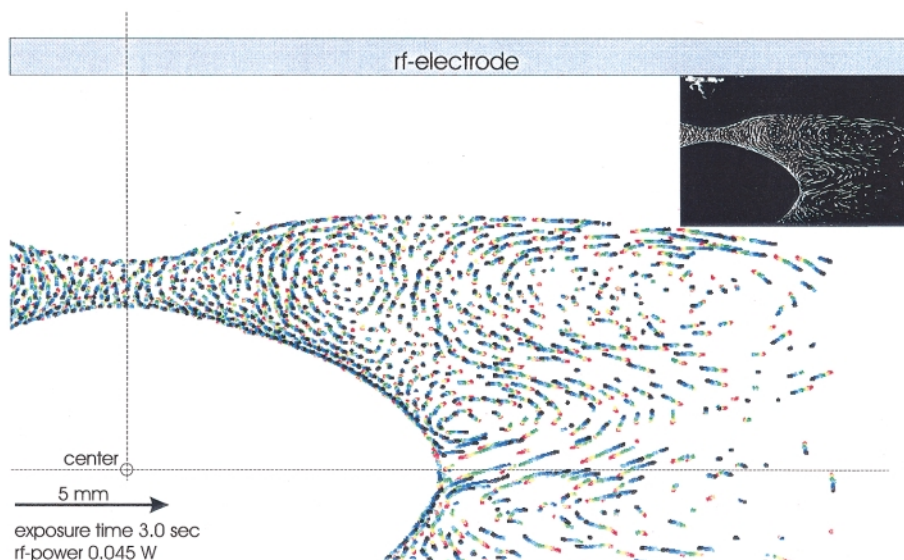
FIG. 2 (color).   Cross sectional view through the colloidal plasma condensation in microgravity (TEXUS 35 rocket flight).   The position of the upper rf electrode, the axis of the chamber and the midplane between the electrodes are indicated (see viewing geometry of Fig. 1).   The rf power was 0.045 W and 150 video images with a total exposure of 3.0 sec are combined and color coded, thus tracing the particle trajectories (beginning with "red").   In the inset the original video image is shown.   Horizontal scans verified that the particle cloud is rotationally symmetric about the chamber axis, with its outer boundary following approximately the calculated equipotential surface in the rf discharge chamber.   It contains about 10^6 microspheres with a characteristic mean separation of ~ 300 μm.   In the center there is a spheroidal "void," where no microspheres are seen.

and not overdamped.   The ratio of the force is calculated to be 3.1 ± 0.3.   The vortex flow direction is compatible with this force gradient at least for the higher rf powers of 0.07 and 0.2 W (Figs. 3 and 4).

When the rf power is reduced (Fig. 2), the size of the void diminishes and the ordered vortex flow breaks up into several smaller vortices.   Typical diameters of these fluid cells range from 10 to 18 particle spacings, suggesting 5 to 9 revolving particle layers.   Whether this has any significance (preferred size) is not clear at this stage.   In any case, the coupling parameter Γ can be determined using the interaction between the fluid cells. At the boundary between these cells we may assume force equilibrium normal to the flow, so that the dimensionless number

$$M_{cp} \equiv \text{centrifugal force/pressure force}$$
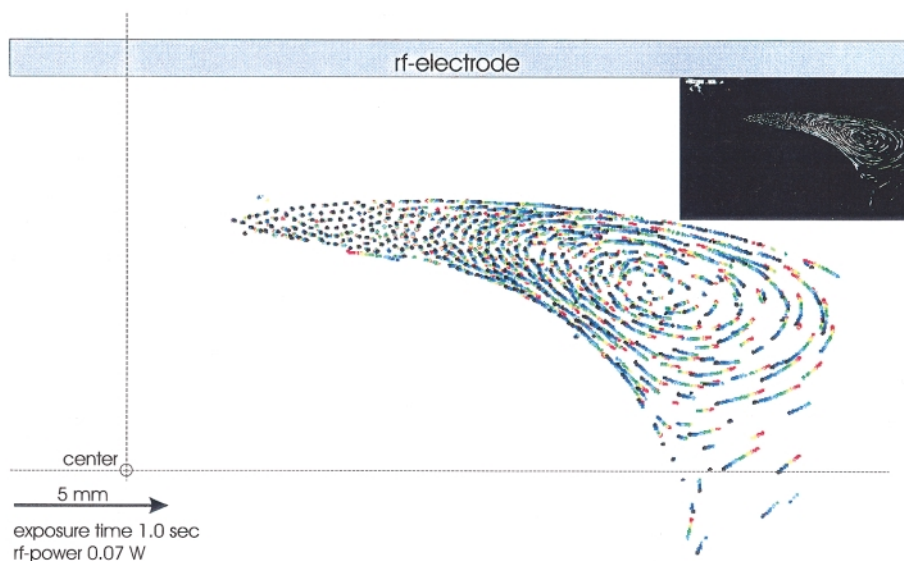$$= 2m\omega^2 R/(kT\Gamma/\Delta) = 1. \qquad (3)$$

FIG. 3 (color).   Cross sectional view through the colloidal plasma condensation, as in Fig. 2, but for an exposure time of 1 sec and for a rf power 0.07 W.
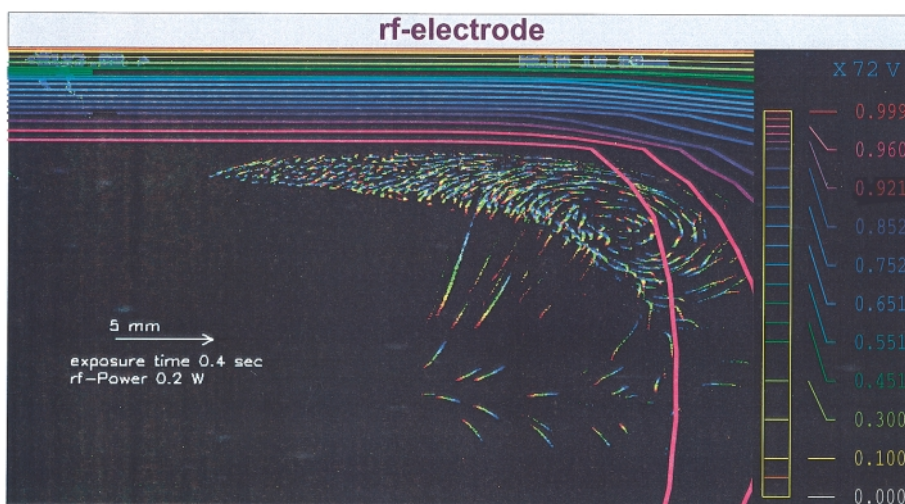
FIG. 4 (color).   Cross sectional view through the colloidal plasma condensation, as in Fig. 2, but for an exposure time of 0.4 sec and for a rf power 0.20 W. Trajectories of single particles inside the void are also depicted. Note that the typical length of the "inner" trajectories (near the chamber midplane) is significantly smaller than that of the "outer" trajectories—suggesting that the force acting on the particles increases with distance from the midplane.

The radius of curvature, R, can be measured, as can $\omega = v_t/R$ (where v_t is the tangential velocity) and Δ. T is 300 K. From the observations we obtain coupling parameters, Γ, of 6.6 and 4.9, respectively, i.e., the plasma condensation is in the strongly coupled Coulomb liquid state.

As the rf power is increased, parts of the system can be made to crystallize (Fig. 3) and the fluid cells merge into one larger one, which rotates faster. Using expression (3) at the boundary between the crystalline and fluid regimes, without the factor 2, gives $\Gamma = 380$, compatible with the observed fact that local crystallization has taken place. The charge on the particles in the crystalline regime can then be estimated at $Q = 1.2 \times 10^3 e$.

In summary, both liquid and crystalline plasma condensations were observed in this microgravity experiment; the strongly coupled "liquid plasma" exhibits ordered flows, boundary interactions, vortices, and in addition viscous diffusion and dissipation (not discussed here). In the absence of gravity, other forces (in particle, it would appear, the thermophoretic force) dominate, leading to new and unexpected phenomena, such as the observed "void."

[1] H. Thomas, G.E. Morfill, V. Demmel, J. Goree, B. Feuerbacher, and D. Möhlmann, Phys. Rev. Lett. **73**, 652–655 (1994).

[2] J.H. Chu and I. Lin, Phys. Rev. Lett. **72**, 4009–4012 (1994).

[3] Y. Hayashi and K. Tachibana, Jpn. J. Appl. Phys. **33**, L804–L806 (1994).

[4] A. Melzer, T. Trottenberg, and A. Piel, Phys. Lett. A **191**, 301–308 (1994).

[5] V.E. Fortov, A.P. Nefedov, O.F. Petrov, A.A. Samarian, and A.V. Chernyschev, Phys. Rev. E **54**, 2236 (1996).

[6] H.M. Thomas and G.E. Morfill, Nature (London) **379**, 806–809 (1996).

[7] I. Lin, W.T. Juan, C.H. Chiang, and J.H. Chu, Science **272**, 1626 (1996).

[8] A. Melzer, A. Homann, and A. Piel, Phys. Rev. E **53**, 2757–2766 (1996).

[9] V.E. Fortov, A.P. Nefedov, O.F. Petrov, A.A. Samarian, and A.V. Chernyschev, Phys. Lett. A **219**, 89 (1996).

[10] H. Ikezi, Phys. Fluids **29**, 1764–1766 (1986).

[11] G.E. Morfill et al., "Plasma Crystal, Columbus Precursor Flights Proposal, ESA" (1991).

[12] Sir J. Maddox, Nature (London) **370**, 411 (1994).

[13] V.N. Tsytovich, Phys.-Usp. **40**, 53–94 (1997).

[14] G. Morfill, H.M. Thomas, and M. Zuzic, *Advances in Dusty Plasmas,* edited by P.K. Shukla, D.A. Mendis, and T. Desai (World Scientific, Singapore, 1997), pp. 99–142.

[15] V.N. Tsytovich, Ya.K. Khodataev, and R. Bingham, Comments Plasma Phys. Control. Fusion **17**, 249–265 (1996).

[16] S. Hamaguchi et al., Phys. Rev. E **56**, 4671–4682 (1997).

[17] G. Morfill and E. Grün, Planet. Space Sci. **27**, 1269 (1979).

[18] J.P. Boeuf and L.C. Pitchford, Phys. Rev. E **51**, 1376 (1995).